Available online at www.sciencedirect.com
ScienceDirect
Journal of Biotechnology 131 (2007) 45–56
Journal of BIOTECHNOLOGY
www.elsevier.com/locate/jbiotec

Kinetic modeling and sensitivity analysis of acetone–butanol–ethanol production

Hideaki Shinto [a], Yukihiro Tashiro [a], Mayu Yamashita [a], Genta Kobayashi [b,*], Tatsuya Sekiguchi [c], Taizo Hanai [d], Yuki Kuriya [d], Masahiro Okamoto [d,e], Kenji Sonomoto [a,f]

[a] *Laboratory of Microbial Technology, Department of Bioscience and Biotechnology, Faculty of Agriculture, Kyushu University, 6-10-1 Hakozaki, Higashi-ku, Fukuoka 812-8581, Japan*
[b] *Laboratory of Microbial Technology, Ariake Sea Research Project, Saga University, 1 Honjo-cho, Saga 840-8502, Japan*
[c] *Department of Information Engineering, Faculty of Engineering, Maebashi Institute of Technology, 460-1 Kamisadorimachi, Maebashi 370-0816, Japan*
[d] *Laboratory for Bioinformatics, Graduate School of Systems Life Sciences, Kyushu University, 6-10-1 Hakozaki, Higashi-ku, Fukuoka 812-8581, Japan*
[e] *Laboratory of Bio-Process Design, Department of Bio-Systems Design, Bio-Architecture Center, Kyushu University, 6-10-1 Hakozaki, Higashi-ku, Fukuoka 812-8581, Japan*
[f] *Laboratory of Functional Food Design, Department of Functional Metabolic Design, Bio-Architecture Center, Kyushu University, 6-10-1 Hakozaki, Higashi-ku, Fukuoka 812-8581, Japan*

Received 22 October 2006; received in revised form 28 April 2007; accepted 16 May 2007

Abstract

A kinetic simulation model of metabolic pathways that describes the dynamic behaviors of metabolites in acetone–butanol–ethanol (ABE) production by *Clostridium saccharoperbutylacetonicum* N1-4 was proposed using a novel simulator WinBEST-KIT. This model was validated by comparing with experimental time-course data of metabolites in batch cultures over a wide range of initial glucose concentrations (36.1–295 mM). By introducing substrate inhibition, product inhibition of butanol, activation of butyrate and considering the cessation of metabolic reactions in the case of insufficiency of energy after glucose exhaustion, the revised model showed 0.901 of squared correlation coefficient (r^2) between experimental time-course of metabolites and calculated ones. Thus, the final revised model is assumed to be one of the best candidates for kinetic simulation describing dynamic behavior of metabolites in ABE production. Sensitivity analysis revealed that 5% increase in reaction of reverse pathway of butyrate production (R_{17}) and 5% decrease in reaction of CoA transferase for butyrate (R_{15}) highly contribute to high production of butanol. These system analyses should be effective in the elucidation which pathway is metabolic bottleneck for high production of butanol.

Keywords: Acetone–butanol–ethanol production; *Clostridium saccharoperbutylacetonicum* N1-4; WinBEST-KIT; Kinetic model; On–off mechanism; Sensitivity analysis

1. Introduction

Metabolic engineering aims at improving the metabolic capabilities of industrially relevant microorganisms during their cultivation (Bailey, 1991; Stephanopoulos and Vallino, 1991). Metabolic pathway modeling is one of the most successful scientific approaches for achieving this task. Metabolic flux analysis (MFA), a systematic method developed to assess the roles of individual steps in a metabolic pathway network, is a great contribution of metabolic engineering (Vallino and Stephanopoulos, 1993). Vallino and Stephanopoulos developed a stoichiometric model of metabolic pathway of *Corynebacterium glutamicum* during growth and lysine synthesis to calculate intracellular fluxes. These calculations are based on the measurements of substrate uptake from a medium, the secretion of products from cells, and the cell growth rate. Using MFA, many studies have recently been conducted to analyze metabolic pathways (Berríos-Rivera et al., 2002; Granström et al., 2002; Koffas et

* Corresponding author. Tel.: +81 952 28 8496; fax: +81 952 28 8496.
E-mail address: gentak@cc.saga-u.ac.jp (G. Kobayashi).

0168-1656/$ – see front matter © 2007 Elsevier B.V. All rights reserved.
doi:10.1016/j.jbiotec.2007.05.005

Nomenclature

[AACoA] acetoacetyl-CoA concentration (mM)
[Acetate] acetate concentration (mM)
[Acetoacetate] acetoacetate concentration (mM)
[Acetone] acetone concentration (mM)
[ACoA] acetyl-CoA concentration (mM)
[BCoA] butyryl-CoA concentration (mM)
[Biomass] biomass concentration (mM)
[Butanol] butanol concentration (mM)
[Butyrate] butyrate concentration (mM)
[CO_2] CO_2 concentration (mM)
[Ethanol] ethanol concentration (mM)
F switching factor of on–off mechanism
[F6P] fructose 6-phosphate concentration (mM)
[Glucose] glucose concentration (mM)
[G3P] glyceraldehyde 3-phosphate concentration (mM)
[Lactate] lactate concentration (mM)
[Pyruvate] pyruvate concentration (mM)
k_j reaction rate constant (h^{-1}) where j is number of corresponding reaction in Fig. 1
K_{aj} activation constant for activator (mM) where j is number of corresponding reaction in Fig. 1
K_{iij} inhibition constant for inhibitor (mM) where j is number of corresponding reaction in Fig. 1
K_{isj} inhibition constant for substrate (mM) where j is number of corresponding reaction in Fig. 1
K_{mj} concentration of metabolite where the rate is equal to half of V_{max} (mM) where j is number of corresponding reaction in Fig. 1
r_j rate equation of metabolic reaction where j is number of corresponding reaction in Fig. 1
R_j metabolic reaction where j is number of corresponding reaction in Fig. 1
V_{maxj} maximum reaction rate (h^{-1}) where j is number of corresponding reaction in Fig. 1

al., 2003; Woldman and Appling, 2002) and to optimize cultivation processes (Shimizu et al., 1999). However, since MFA based on a stoichiometric model is so called "a snapshot" of the metabolic flux at a steady state and does not provide any temporal or time variant information, it is impossible to simulate the dynamic behavior of metabolites. On the other hand, a kinetic simulation model of metabolic pathways that describes the dynamic behavior of metabolites is efficient for creating the optimal design of bioreactors and developing operation strategies with minimum exertion. Furthermore, sensitivity analysis by the kinetic simulation model could reveal which pathways have impact on high production of target products. To date, some studies have been conducted on creating optimal designs of bioreactors and developing operation strategies by using a kinetic simulation model (Hodge and Karim, 2002; Rizzi et al., 1997); however, the development of such a model is difficult because many kinetic parameters need to be estimated in the model. Moreover, this becomes even more difficult because no kinetic simulation models including complicated metabolic pathways have been developed in several microorganisms.

The metabolic pathways of acetone–butanol–ethanol (ABE)-producing clostridia comprise two distinct characteristic phases, namely, acidogenesis and solventogenesis. A diagrammatic representation of the metabolic pathways of *Clostridium acetobutylicum* ATCC824^T by Jones and Woods (1986) is summarized in Fig. 1. Typically, during acidogenesis, a cell grows exponentially, acetic acid and butyric acid are produced with ATP formation. In addition, in the solventogenesis that follows, the cell growth attains a stationary phase; organic acids are reassimilated; and acetone, butanol, and ethanol are produced. ABE cultivation includes substrate inhibition by glucose and product inhibition by butanol (Jones and Woods, 1986; Soni et al., 1987); these lead to low productivity and yield of solvents. On the other hand, Tashiro et al. (2004) have experimentally shown the acceleration of butanol production by feeding butyrate. As just described, ABE-producing clostridia possess complicated metabolic function.

Since the metabolic pathway involved in ABE production is quite complicated, very few models describing this pathway have been published. Papoutsakis (1984) developed a stoichiometric model for this pathway; this model could be used to calculate or estimate the rates of reactions occurring within the pathway in several ABE-producing clostridia. Desai et al. (1999) analyzed the contribution of acid formation pathways in the metabolism of *C. acetobutylicum* ATCC824^T by using MFA. However, there is no report on the development of a kinetic simulation model for describing the dynamic behavior of metabolites in ABE production.

In order to successfully create an optimal design for bioreactors and develop operation strategies for ABE production and reveal the metabolic network in detail, we developed a kinetic simulation model of metabolic pathways in this study. We consider the following three points when developing this model for ABE production in *Clostridium saccharoperbutylacetonicum* N1-4 ATCC13564: (1) the model should describe the dynamic behaviors of metabolites involved in ABE production, (2) it should describe inhibitory and activatory mechanism, and (3) it should be able to realize experimental data obtained over a wide range of initial glucose concentrations. Furthermore, we carried out sensitivity analysis to assess its validity and to reveal which pathways have impact on high production of butanol.

2. Materials and methods

2.1. Bacterial strain

C. saccharoperbutylacetonicum N1-4 ATCC13564 was used in this study (Ishizaki et al., 1999). The culture was maintained in the form of spores in fresh potato glucose (PG) medium at 4 °C. To prepare the seed culture, 1 ml of spore suspension was aseptically transferred into 9 ml of PG medium. Next, this admixture was subjected to heat-shock by placing it in boiling water for 1 min and was subsequently cultivated at 30 °C for 24 h (Lee et al., 1995).

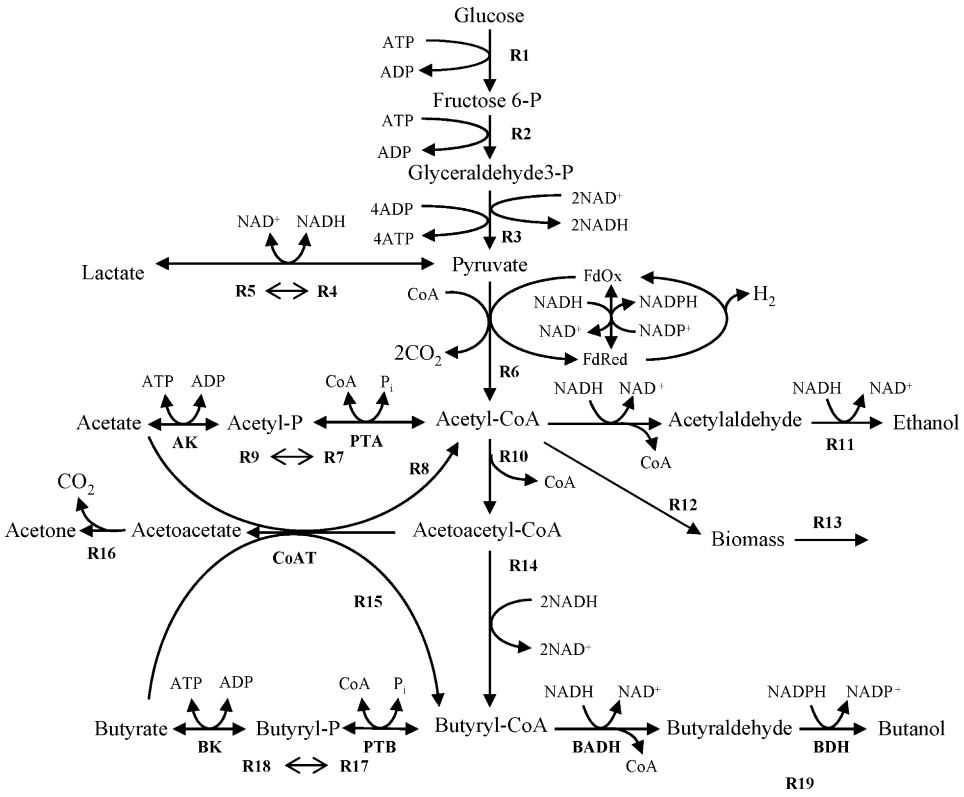

Fig. 1. Metabolic pathways in *C. acetobutylicum* ATCC824^T. Enzymes are indicated in bold and abbreviated as follows: PTA, phosphotransacetylase; AK, acetate kinase; CoAT, CoA transferase; PTB, phosphotransbutyrylase; BK, butyrate kinase; BADH, butyraldehyde dehydrogenase; BDH, butanol dehydrogenase.

2.2. Media

Tryptone-yeast extract-acetate (TYA) medium was used for the pre-culture and main culture. The composition of this medium per liter of distilled water (Ishizaki et al., 1999) is as follows: 5–50 g glucose, 2 g yeast extract, 6 g tryptone, 3 g CH_3COONH_4, 0.3 g $MgSO_4{\cdot}7H_2O$, 0.5 g KH_2PO_4, and 10 mg $FeSO_4{\cdot}7H_2O$. In all experiments, the initial pH of the medium was adjusted to 6.5 with 1 M NaOH and the medium was sterilized at 115 °C for 15 min.

2.3. Batch culture conditions over a wide range of initial glucose concentrations

A batch culture was carried out statically at 30 °C in a 500 ml Erlenmeyer flask with initial glucose concentrations of 36.1, 70.6, 122, and 295 mM (6.50, 12.7, 22.0, and 53.1 g l^{-1}, respectively) with a 300 ml working volume that included a 10% inoculum size. After inoculation, the broth was sparged with filtered oxygen-free nitrogen gas to maintain strict anaerobic conditions. Samples were periodically withdrawn. We carried out cultivation two times to assess its reproducibility.

2.4. Analytical methods

The cell concentration was estimated by measuring the optical density (OD) with a spectrophotometer (V-530; JASCO, Tokyo, Japan), and the dry cell weight (DCW) was calculated using a predetermined correlation between OD at 562 nm and DCW. The concentration of organic acids, solvents, and glucose in the supernatant were determined by the method described previously (Tashiro et al., 2004).

2.5. Model development

Modeling and simulation were conducted using WinBEST-KIT (Biochemical Engineering System analyzing Tool-KIT (Windows version)) (Okamoto et al., 1997; Sekiguchi and Okamoto, 2006; Yoshimura et al., 2003). WinBEST-KIT mainly comprises a module known as "MassAction++" that enables to construct and analyze a reaction scheme that is represented by both mass action law (mass balance) and approximate velocity function of enzyme kinetics. The simultaneous differential equations were numerically calculated by the Gear method (Gear, 1971), which is one of the most efficient numerical calculation methods for "stiff" differential equations.

A kinetic simulation model of metabolic pathway was developed by considering the substrate utilization rate, production rate, and cell growth rate. The simulation model was based on the metabolic pathways of *C. acetobutylicum* ATCC824^T (Jones and Woods, 1986) (Fig. 1). The rate equations of each metabolic reaction in Fig. 1 can be represented as follows:

$$r_1 = \frac{V_{\max 1}[\text{Glucose}][\text{Biomass}]}{K_{\text{m1}} + [\text{Glucose}]} \times F \quad (1)$$

$$r_2 = \frac{V_{\max 2}[\text{F6P}][\text{Biomass}]}{K_{\text{m2}} + [\text{F6P}]} \times F \quad (2)$$

$$r_3 = \frac{V_{\max 3}[\mathrm{G3P}][\mathrm{Biomass}]}{K_{\mathrm{m}3} + [\mathrm{G3P}]} \times F \quad (3)$$

$$r_4 = \frac{V_{\max 4}[\mathrm{Lactate}][\mathrm{Biomass}]}{K_{\mathrm{m}4} + [\mathrm{Lactate}]} \times F \quad (4)$$

$$r_5 = \frac{V_{\max 5}[\mathrm{Pyruvate}][\mathrm{Biomass}]}{K_{\mathrm{m}5} + [\mathrm{Pyruvate}]} \times F \quad (5)$$

$$r_6 = \frac{V_{\max 6}[\mathrm{Pyruvate}][\mathrm{Biomass}]}{K_{\mathrm{m}6} + [\mathrm{Pyruvate}]} \times F \quad (6)$$

$$r_7 = \frac{V_{\max 7}[\mathrm{Acetate}][\mathrm{Biomass}]}{K_{\mathrm{m}7} + [\mathrm{Acetate}]} \times F \quad (7)$$

$$r_8 = V_{\max 8}\left(\frac{1}{1 + (K_{\mathrm{m8A}}/[\mathrm{Acetate}])}\right) \times \left(\frac{1}{1 + (K_{\mathrm{m8B}}/[\mathrm{AACoA}])}\right)[\mathrm{Biomass}] \quad (8)$$

$$r_9 = \frac{V_{\max 9}[\mathrm{ACoA}][\mathrm{Biomass}]}{K_{\mathrm{m}9} + [\mathrm{ACoA}]} \times F \quad (9)$$

$$r_{10} = \frac{V_{\max 10}[\mathrm{ACoA}][\mathrm{Biomass}]}{K_{\mathrm{m}10} + [\mathrm{ACoA}]} \quad (10)$$

$$r_{11} = \frac{V_{\max 11}[\mathrm{ACoA}][\mathrm{Biomass}]}{K_{\mathrm{m}11} + [\mathrm{ACoA}]} \times F \quad (11)$$

$$r_{12} = \frac{V_{\max 12}[\mathrm{ACoA}][\mathrm{Biomass}]}{K_{\mathrm{m}12}(1 + [\mathrm{Butanol}]/K_{\mathrm{ii}12}) + [\mathrm{ACoA}](1 + [\mathrm{Butanol}]/K_{\mathrm{ii}12})} \quad (12)$$

$$r_{13} = k_{13}[\mathrm{Biomass}] \quad (13)$$

$$r_{14} = \frac{V_{\max 14}[\mathrm{AACoA}][\mathrm{Biomass}]}{K_{\mathrm{m}14} + [\mathrm{AACoA}]} \times F \quad (14)$$

$$r_{15} = V_{\max 15}\left(\frac{1}{1 + (K_{\mathrm{m15A}}/[\mathrm{Butyrate}])}\right) \times \left(\frac{1}{1 + (K_{\mathrm{m15B}}/[\mathrm{AACoA}])}\right)[\mathrm{Biomass}] \quad (15)$$

$$r_{16} = \frac{V_{\max 16}[\mathrm{Acetoacetate}][\mathrm{Biomass}]}{K_{\mathrm{m}16} + [\mathrm{Acetoacetate}]} \quad (16)$$

$$r_{17} = \frac{V_{\max 17}[\mathrm{Butyrate}][\mathrm{Biomass}]}{K_{\mathrm{m}17} + [\mathrm{Butyrate}]} \times F \quad (17)$$

$$r_{18} = \frac{V_{\max 18}[\mathrm{BCoA}][\mathrm{Biomass}]}{K_{\mathrm{m}18} + [\mathrm{BCoA}]} \times F \quad (18)$$

$$r_{19} = \frac{V_{\max 19}[\mathrm{BCoA}][\mathrm{Biomass}]}{K_{\mathrm{m}19} + [\mathrm{BCoA}]} \times F \quad (19)$$

Since the acetoacetyl-CoA transferase (CoAT) exhibits a broad carboxylic acid specificity and can catalyze the transfer of CoA to either acetate and butyrate (Boynton et al., 1994), the rate equations of CoAT were developed separately (Eq. (8), Eq. (15)). The rate equations of CoAT consisted of the reaction of random bi bi. Since Soni et al. (1987) have reported that butanol inhibits cell growth, we developed rate equation of cell growth (Eq. (12)) at Michaelis–Menten type kinetics with noncompetitive inhibition. The reaction balance of target metabolites can be represented as follows:

$$\frac{\mathrm{d}[\mathrm{Glucose}]}{\mathrm{d}t} = -r_1 \quad (20)$$

$$\frac{\mathrm{d}[\mathrm{F6P}]}{\mathrm{d}t} = r_1 - r_2 \quad (21)$$

$$\frac{\mathrm{d}[\mathrm{G3P}]}{\mathrm{d}t} = r_2 - r_3 \quad (22)$$

$$\frac{\mathrm{d}[\mathrm{Pyruvate}]}{\mathrm{d}t} = r_3 + r_4 - r_5 - r_6 \quad (23)$$

$$\frac{\mathrm{d}[\mathrm{Lactate}]}{\mathrm{d}t} = r_5 - r_4 \quad (24)$$

$$\frac{\mathrm{d}[\mathrm{ACoA}]}{\mathrm{d}t} = r_6 + r_7 + r_8 - r_9 - r_{10} - r_{11} - r_{12} \quad (25)$$

$$\frac{\mathrm{d}[\mathrm{Biomass}]}{\mathrm{d}t} = r_{12} - r_{13} \quad (26)$$

$$\frac{\mathrm{d}[\mathrm{Acetate}]}{\mathrm{d}t} = r_9 - r_7 - r_8 \quad (27)$$

$$\frac{\mathrm{d}[\mathrm{Ethanol}]}{\mathrm{d}t} = r_{11} \quad (28)$$

$$\frac{\mathrm{d}[\mathrm{AACoA}]}{\mathrm{d}t} = r_{10} - r_8 - r_{14} - r_{15} \quad (29)$$

$$\frac{\mathrm{d}[\mathrm{Acetoacetate}]}{\mathrm{d}t} = r_8 + r_{15} - r_{16} \quad (30)$$

$$\frac{\mathrm{d}[\mathrm{BCoA}]}{\mathrm{d}t} = r_{14} + r_{15} + r_{17} - r_{18} - r_{19} \quad (31)$$

$$\frac{\mathrm{d}[\mathrm{Butyrate}]}{\mathrm{d}t} = r_{18} - r_{15} - r_{17} \quad (32)$$

$$\frac{\mathrm{d}[\mathrm{Acetone}]}{\mathrm{d}t} = r_{16} \quad (33)$$

$$\frac{\mathrm{d}[\mathrm{CO_2}]}{\mathrm{d}t} = r_6 + r_{16} \quad (34)$$

$$\frac{\mathrm{d}[\mathrm{Butanol}]}{\mathrm{d}t} = r_{19} \quad (35)$$

The rate equation $-r_{13}$ in Eq. (26) indicated death reaction of the cell. We named this model as Model I. The value of F was set at 1 in Model I.

It has been reported that butanol inhibits glucose utilization and butanol production in ABE cultivation (Jones and Woods, 1986; Soni et al., 1987) and that an increase in the initial glucose concentration results in the inhibition of glucose utilization, thereby leading to a longer cultivation time in *C. saccharoperbutylacetonicum* N1-4 (data not shown). Furthermore, Tashiro et al. (2004) have experimentally shown the acceleration of butanol production by feeding butyrate. Therefore, we introduced these inhibition and activation terms to a revised version of Model I

Table 1
Initial values of each metabolite for a determination of kinetic parameters and a validity of the estimated kinetic parameters with initial glucose concentrations of 36.1, 70.6, 122, and 295 mM

Glucose (mM)	Biomass (mM)	Acetate (mM)	Acetone (mM)	Butyrate (mM)	Butanol (mM)
36.1	1.34	41.6	0	1.92	3.01
70.6	1.53	40.0	2.00	1.95	3.83
122	1.36	46.5	0	3.98	2.90
295	1.41	41.2	2.88	1.00	4.49

(the model with considering butanol inhibition to cell growth) and named it as Model II. The value of F was set at 1 in Model II. In Model II, r_1, r_{17}, and r_{19} (given below) were substituted as follows:

$$r_1 = \frac{V_{\max 1}[\text{Glucose}][\text{Biomass}]}{K_{\text{m1}}(1 + [\text{Glucose}]/K_{\text{is1}}) + [\text{Glucose}](1 + [\text{Butanol}]/K_{\text{ii1}})} \times F \quad (36)$$

$$r_{17} = \frac{V_{\max 17}[\text{Butyrate}][\text{Biomass}]}{K_{\text{m17}}(1 + K_{\text{a17}}/[\text{Butyrate}]) + [\text{Butyrate}]} \times F \quad (37)$$

$$r_{19} = \frac{V_{\max 19}[\text{BCoA}][\text{Biomass}]}{K_{\text{m19}}(1 + K_{\text{a19}}/[\text{Butyrate}]) + [\text{BCoA}](1 + [\text{Butanol}]/K_{\text{ii19}})} \times F \quad (38)$$

In Model II, the rate equation of r_1 (Eq. (36)) was developed by combining the substrate inhibition by glucose and uncompetitive inhibition by butanol. The rate equation of r_{17} (Eq. (37)) was developed using the specific activation by butyrate. The rate equation of r_{19} (Eq. (38)) was also developed by combining the uncompetitive inhibition by butanol and specific activation by butyrate.

2.6. Introduction of on–off mechanism

Since many metabolic reactions in ABE production occur in the presence of ATP or NADH (Fig. 1), these reactions may terminate when there is an insufficiency of energy, i.e., after the exhaustion of glucose. In consideration of the cessation of metabolic reactions after glucose exhaustion, an on–off mechanism (Okamoto et al., 1988) was introduced into Model II. In this mechanism, we assumed F whose value is 1 or 0 depending on the glucose concentration in the broth. Since on–off mechanism could not drive when the concentration of changing point was set at 0 (Okamoto et al., 1988), the concentration of changing point was set at 1.00 mM, sufficiently low concentration; its value was assumed to be 1 when glucose concentration is over 1.00 mM and 0 when it is under 1.00 mM. This on–off mechanism was introduced into equations (Eqs. (1)–(7), (9), (11), (14), (17)–(19), (36)–(38)) of metabolic reactions that were accompanied with ATP, ADP, NADH, or NAD^+ (Fig. 1). We named this model as Model III.

2.7. Determination of model parameters

Microbial biomass could be expressed as $CH_pO_nN_q$ (Papoutsakis, 1984). The content ratio of C, H, O, and N of *C. saccharoperbutylacetonicum* N1-4 was measured using an absorptiometer to obtain the average molecular weight of the strain. The average molecular weight of the biomass was set to 172. The values of the kinetic parameters were estimated by heuristic searching to realize the experimental data of batch culture of *C. saccharoperbutylacetonicum* N1-4 with the initial glucose concentration of 70.6 mM. The initial value of metabolite was set as shown in Table 1. In Model II, the values of k_j, $V_{\max j}$, $K_{\text{m}j}$, and $K_{\text{ii}12}$ were same with Model I, and only the value of $K_{\text{a}j}$, $K_{\text{ii}j}$, and $K_{\text{is}j}$ were estimated. In Model III, the values of kinetic parameters were same with Model II. To confirm the validity of the estimated values of the kinetic parameters in Model III, we compared the calculated time-courses with experimental data obtained at initial glucose concentrations of 36.1, 122, and 295 mM. The average squared correlation coefficients (r^2) between simulation results and experimental data were calculated to quantitatively determine the accuracy of the models.

2.8. Sensitivity analysis

Sensitivity analysis was carried out to assess the validity of developed model and to reveal which pathway has most impact and is significant for high production of butanol. This study assessed the impact on endpoint butanol production, amount of butanol production, and butanol productivity given a 5% increase in each kinetic parameter (Table 2) in rate equations in Model III with initial glucose concentrations of 70.6 mM.

First of all, we assessed the following endpoint deviation (ED) of butanol to reveal which reaction pathway has impact on butanol production:

$$\text{ED} = 100 \times \frac{[\text{Butanol}]_{\text{end 5\%}} - [\text{Butanol}]_{\text{end control}}}{[\text{Butanol}]_{\text{end control}}} \quad (39)$$

where $[\text{Butanol}]_{\text{end 5\%}}$ was butanol concentration at 60 h given a 5% increase in each kinetic parameter in rate equations and $[\text{Butanol}]_{\text{end control}}$ was butanol concentration at 60 h by Model III.

Secondly, we assessed integral deviation (ID), Eq. (41) and integral absolute deviation (IAD), Eq. (42) of butanol to reveal the type of temporal profile in Fig. 2 by a 5% increase in each kinetic parameter.

The average area of butanol production at time t (h) to $t+1$ (h) (ABP_t) can be represented as follows:

$$\text{ABP}_t = \frac{([\text{Butanol}]_t + [\text{Butanol}]_{t+1}) \times (t + 1 - t)}{2} = \frac{[\text{Butanol}]_t + [\text{Butanol}]_{t+1}}{2} \quad (40)$$

Table 2
Kinetic parameters estimated by comparing with experimental data of 70.6 mM of initial glucose in Models I–III

Reaction	k[a] (h^{-1})	V_{max}[a] (h^{-1})	K_m[a] (mM)	K_{is}[b] (mM)	K_{ii}[b] (mM)	K_a[b] (mM)	K_{mA}[a] (mM)	K_{mB}[a] (mM)
R_1		3.20	46.0	55.6	67.5			
R_2		40.0	10.0					
R_3		120	26.5					
R_4		7.50	177					
R_5		9.70	500					
R_6		180	1.50					
R_7		0.30	50.0					
R_8		19.0					40.0	70.0
R_9		26.5	51.0					
R_{10}		20.0	1.00					
R_{11}		7.45	30.0					
R_{12}		8.10	1.10		23.0[a]			
R_{13}	0.017							
R_{14}		10.0	5.20					
R_{15}		80.0					15.0	50.0
R_{16}		12.0	10.0					
R_{17}		35.0	4.90			2.20		
R_{18}		100	6.10					
R_{19}		3.15	5.00		67.5	2.20		

[a] Estimated kinetic parameters in Models I–III.
[b] Estimated kinetic parameters in Models II and III.

where $[\text{Butanol}]_t$ and $[\text{Butanol}]_{t+1}$ were butanol concentration at time t (h) and time $t+1$ (h), respectively.

The integral deviation (ID) from time 0 (h) to 60 (h) and the integral absolute deviation (IAD) during reaction time (0–60 h) can be represented as follows:

$$\text{ID} = 100 \times \sum_{t=0}^{60} \left(\frac{\text{ABP}_{t\,5\%} - \text{ABP}_{t\,\text{control}}}{\text{ABP}_{t\,\text{control}}} \right) \quad (41)$$

$$\text{IAD} = 100 \times \sum_{t=0}^{60} \left(\left| \frac{\text{ABP}_{t\,5\%} - \text{ABP}_{t\,\text{control}}}{\text{ABP}_{t\,\text{control}}} \right| \right) \quad (42)$$

where $\text{ABP}_{t\,5\%}$ was ABP_t given a 5% increase in each kinetic parameter in rate equations and $\text{ABP}_{t\,\text{control}}$ was ABP_t at Model III. The schematic diagram was shown in Fig. 2. As shown in Fig. 2, there are six types of changes in butanol production by a 5% change in each of the parameters in rate equation. In temporal profile (a) in Fig. 2, most positive impact on butanol production, 5% increase of kinetic parameter resulted in higher endpoint butanol production and butanol productivity compared to control. In temporal profile (b), most negative impact on butanol production, 5% increase of kinetic parameter resulted in lower butanol production and productivity compared to control. In temporal profiles (c) and (e), 5% increase of kinetic parameter

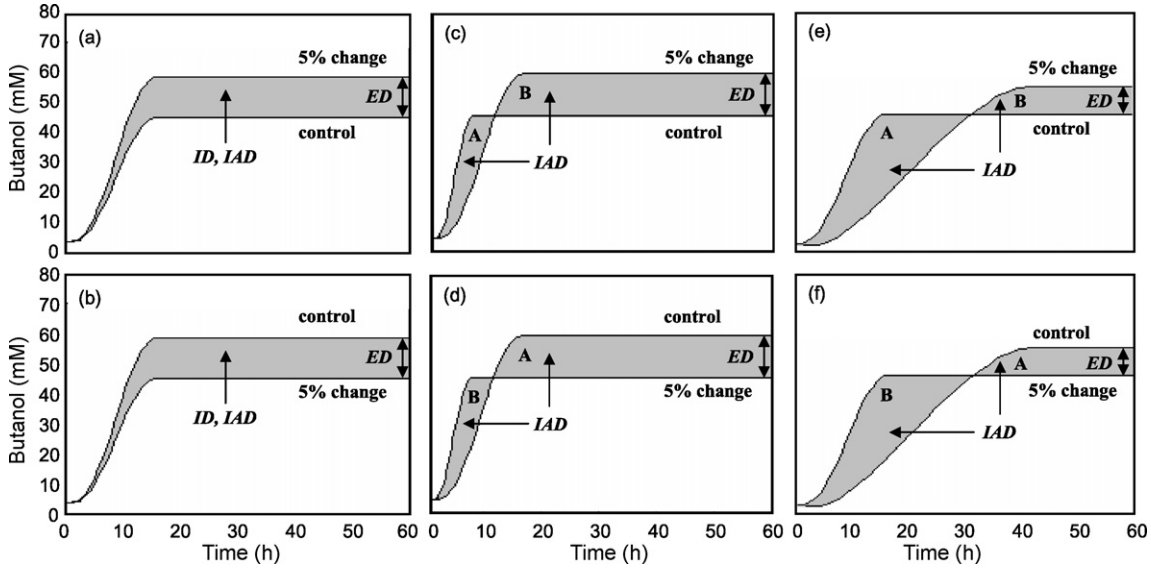

Fig. 2. Schematic diagram of sensitivity analysis. There are six types of temporal profiles in butanol production by a 5% change in each of the parameters in rate equation. (a) ED > 0, ID = IAD > 0, (b) ED < 0, ID < 0, IAD > 0, |ID| = IAD, (c) ED > 0, ID = $B - A$ > 0, IAD = $A + B$, |ID| < IAD, (d) ED < 0, ID = $B - A$ < 0, IAD = $A + B$, |ID| < IAD, (e) ED > 0, ID = $B - A$ < 0, IAD = $A + B$, |ID| < IAD, and (f) ED < 0, ID = $B - A$ > 0, IAD = $A + B$, |ID| < IAD.

resulted in higher butanol production and lower butanol productivity compared to control. In temporal profiles (d) and (f), 5% increase of kinetic parameter resulted in the lower butanol production and higher butanol productivity compared to control. Our preferable target is to get the temporal profiles (a), (c), and (f) for the higher butanol production and butanol productivity, however, the temporal profile (a) is the best.

3. Results

3.1. Batch cultivation

To obtain the experimental data for the development of the kinetic simulation model of metabolic pathway for ABE production by *C. saccharoperbutylacetonicum* N1-4, batch cultures were carried out in TYA medium with initial glucose concentrations of 36.1, 70.6, 122, and 295 mM. As shown in Fig. 3, the solvent production increased with the initial glucose concentration. The maximum butanol production was 26.2, 52.5, 94.2, and 172 mM with initial glucose concentrations of 36.1, 70.6, 122, and 295 mM, respectively. The glucose in the broth was exhausted after 12, 15, 21, and 24 h of cultivation for initial glucose concentrations of 36.1, 70.6, 122, and 295 mM, respectively. After the exhaustion of glucose, both organic acid reassimilation and solvent production terminated due to an insufficiency of energy-rich metabolites such as ATP or NADH. The experimental data gave high reproducible results.

3.2. Effect of inhibition and activation terms

Model I (the model with considering butanol inhibition to cell growth) was developed based on the metabolic pathways of *C. acetobutylicum* ATCC824^T (Fig. 1), and the kinetic parameters in Model I (k_j, $V_{\max j}$, K_{mj}, and K_{ii12}) were estimated to fit the experimental time-course data obtained with the initial glucose concentration of 70.6 mM in *C. saccharoperbutylacetonicum* N1-4. The estimated kinetic parameters were shown in Table 2. The results were shown in Fig. 4. As shown in Table 3, the correlation coefficient (r^2) of each metabolite was calculated

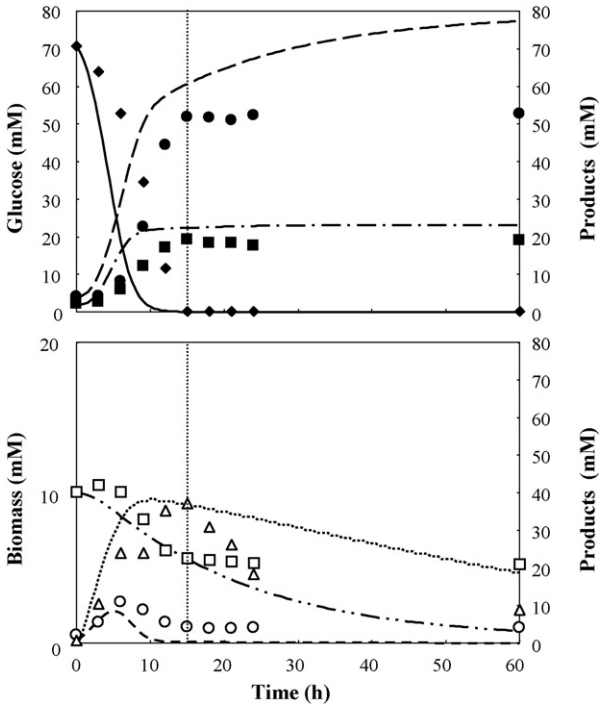

Fig. 4. Experimental time-course data and simulation results of target metabolites with initial glucose concentration of 70.6 mM in Model I. The bold, broken or dotted lines indicate the simulation results and the symbols show the experimental data. Vertical dotted line represents the time point of the exhaustion of glucose in experimental data. The error bars of experimental data have been omitted. —, glucose (sim); – ·· –, acetone (sim); – –, butanol (sim); – · –, acetate (sim); - - - -,·butyrate (sim); · · ·, biomass (sim); ♦, glucose (exp); ■, acetone (exp); ●, butanol (exp); □, acetate (exp); ◯, butyrate (exp); △, biomass (exp).

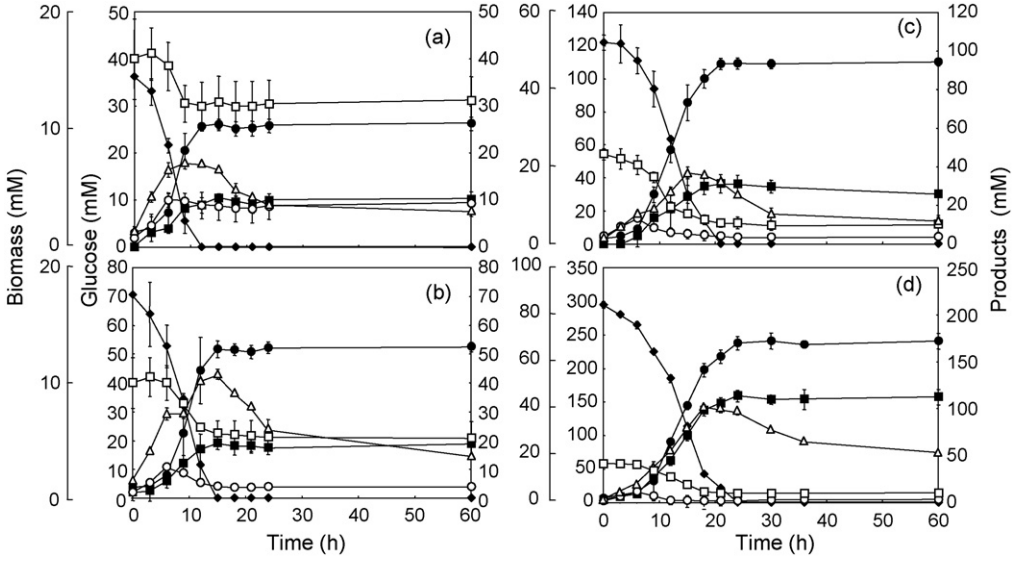

Fig. 3. Experimental time-course data of target metabolites in batch cultures over a wide range of initial glucose concentrations. Initial concentration of glucose; (a) 36.1 mM, (b) 70.6 mM, (c) 122 mM, and (d) 295 mM. The error bars indicate the standard deviations of metabolites ($n = 2$). ♦, glucose; ■, acetone; ●, butanol; □, acetate; ◯, butyrate; △, biomass.

Table 3
Average squared correlation coefficients (r^2) between simulation results and experimental data with initial glucose concentration of 70.6 mM in Models I–III

Model	Biomass	Glucose	Acetate	Acetone	Butyrate	Butanol	Average
I	0.906	0.883	0.915	0.922	0.632	0.942	0.867
II	0.879	0.979	0.893	0.995	0.917	0.981	0.941
III	0.910	0.979	0.987	0.996	0.957	0.993	0.970

to be 0.906 for biomass, 0.883 for glucose, 0.915 for acetate, 0.922 for acetone, 0.632 for butyrate, and 0.942 for butanol; the overall value was 0.867.

Subsequently, the kinetic parameters in Model II, the model with considering both inhibition and activation, were estimated with the initial glucose concentration of 70.6 mM to realize the experimental time-course data. The estimated kinetic parameters were shown in Table 2. In Model II, the values of k_j, $V_{\max j}$, $K_{\mathrm{m}j}$, and $K_{\mathrm{ii}12}$ were same with Model I, and only the value of $K_{\mathrm{a}j}$, $K_{\mathrm{ii}j}$, and $K_{\mathrm{is}j}$ were estimated. As a result, the dynamic behaviors of target metabolites in Model II were qualitatively fitted with the corresponding experimental time-course data until glucose exhaustion (see Fig. 5). The r^2 of each metabolite was calculated to be 0.879 for biomass, 0.979 for glucose, 0.893 for acetate, 0.995 for acetone, 0.917 for butyrate, and 0.981 for butanol; the overall value was 0.941 (see Table 3). The overall value of r^2 increased from 0.867 (Model I) to 0.941 (Model II). These results confirmed that the introduction of inhibition and activation terms into the model improved the simulation results. The simulation results of Models I and II, however, showed that both organic acid reassimilation and solvent production continued even after glucose exhaustion; this is in contradiction with the experimental time-course data (see Figs. 4 and 5). Therefore, we need to revise Model II in order to describe the cessation of related metabolic reactions after glucose exhaustion.

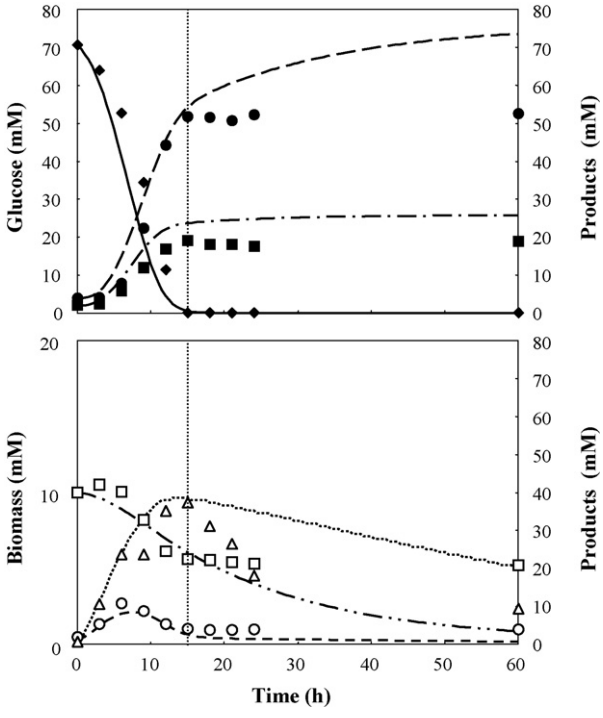

Fig. 5. Experimental time-course data and simulation results of target metabolites with initial glucose concentration of 70.6 mM in Model II. The bold, broken or dotted lines indicate the simulation results and the symbols show the experimental data. Vertical dotted line represents the time point of the exhaustion of glucose in experimental data. The error bars of experimental data have been omitted. —, glucose (sim); – ·· –, acetone (sim); – –, butanol (sim); – · –, acetate (sim); - - - -,·butyrate (sim); ···, biomass (sim); ♦, glucose (exp); ■, acetone (exp); ●, butanol (exp); □, acetate (exp); ◯, butyrate (exp); △, biomass (exp).

3.3. Introduction of on–off mechanism

Model III was designed by introducing an on–off mechanism (Eqs. (1)–(7), (9), (11), (14), (17)–(19)) into Model II, and the kinetic parameters of Model III were estimated to realize the experimental time-course data with the initial glucose concentration of 70.6 mM. The estimated kinetic parameters were shown in Table 2. In Model III, the values of kinetic parameters were same as those in Model II. As shown in Figs. 6(b) and 7(b), in Model III, both organic acid reassimilation and solvent production terminated after glucose exhaustion, which showed qualitative consistency with the experimental time-course data. The average r^2 of each metabolite with the initial glucose concentrations were calculated to be 0.910 for biomass, 0.979 for glucose, 0.987 for acetate, 0.996 for acetone, 0.957 for butyrate, and 0.993 for butanol, and 0.970 for total (see Table 3). The average r^2 for total increased from 0.941 (Model II) to 0.970 (Model III). Furthermore, to confirm the validity of Model III, the simulation results were compared with the experimental time-course data for initial glucose concentrations of 36.1, 122, and 295 mM. As shown in Figs. 6 and 7, the simulation results showed qualitative consistency with the experimental time-course data. The average r^2 of each metabolite with the initial glucose concentrations were calculated to be 0.850 for biomass, 0.972 for glucose, 0.970 for acetate, 0.983 for acetone, 0.644 for butyrate, 0.984 for butanol, and 0.901 for total (see Table 4). Thus, Model III is one of the best model-candidates of ABE production that can realize the experimentally obtained time-course data of the target metabolites over a wide range of initial glucose concentration.

3.4. Sensitivity analysis

Sensitivity analysis was carried out to assess the impact on endpoint butanol production, amount of butanol production, and butanol productivity given a 5% increase in each kinetic parameter in rate equations. The endpoint deviation (ED, Eq. (39)), the integral deviation (ID, Eq. (41)), and the integral absolute deviation (IAD, Eq. (42)) were presented in Table 5. In the case of either higher ED or ID (>0.03) in Table 5, the temporal profile with a 5% increase in each kinetic parameter was examined.

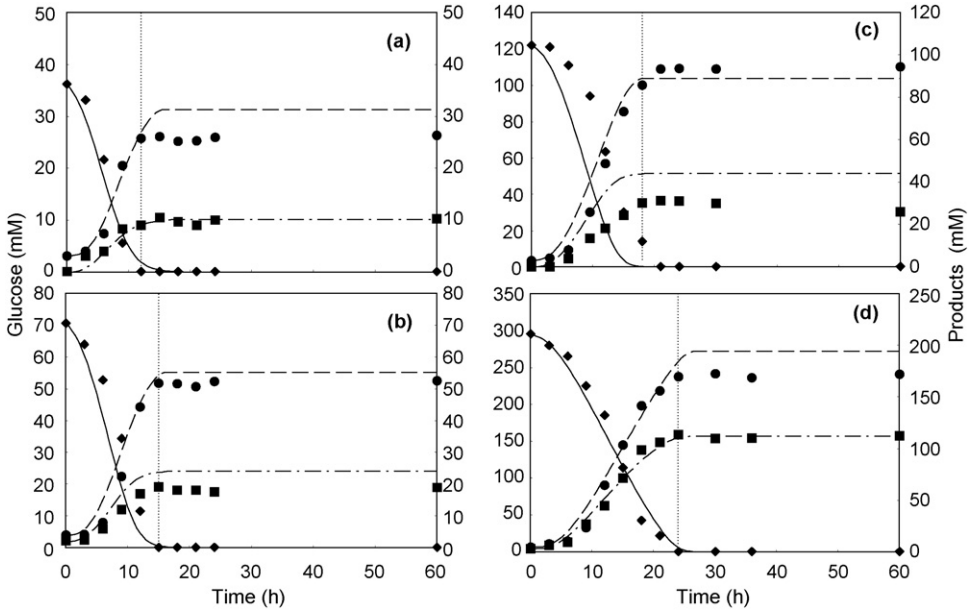

Fig. 6. Experimental time-course data and simulation results of glucose, acetone, and butanol in Model III. Initial concentration of glucose; (a) 36.1 mM, (b) 70.6 mM, (c) 122 mM, and (d) 295 mM. The bold, broken or dotted lines indicate the simulation results and the symbols show the experimental data. Vertical dotted line represents the time point of the exhaustion of glucose in experimental data. The error bars of experimental data have been omitted. —, glucose (sim); – · –, acetone (sim); – –, butanol (sim); ♦, glucose (exp); ■, acetone (exp); ●, butanol (exp).

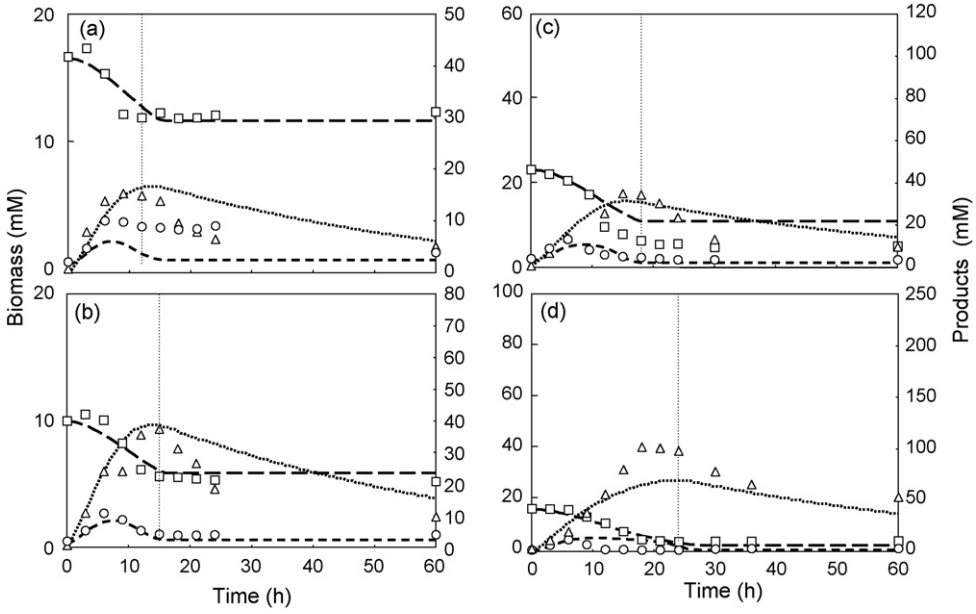

Fig. 7. Experimental time-course data and simulation results of acetate, butyrate, and biomass in Model III. Initial concentration of glucose; (a) 36.1 mM, (b) 70.6 mM, (c) 122 mM, and (d) 295 mM. The bold, broken or dotted lines indicate the simulation results and the symbols show the experimental data. Vertical dotted line represents the time point of the exhaustion of glucose in experimental data. The error bars of experimental data have been omitted. – – –, acetate (sim); - - -,·butyrate (sim); · · ·, biomass (sim); □, acetate (exp); ◯, butyrate (exp); △, biomass (exp).

Table 4
Average squared correlation coefficients (r^2) between simulation results and experimental data with initial glucose concentration of 36.1, 70.6, 122, and 295 mM in Model III

Initial glucose (mM)	Biomass	Glucose	Acetate	Acetone	Butyrate	Butanol	Average
36.1	0.651	0.995	0.908	0.976	0.424	0.977	0.822
70.6	0.910	0.979	0.987	0.996	0.957	0.993	0.970
122	0.895	0.924	0.991	0.969	0.801	0.971	0.925
295	0.945	0.990	0.994	0.992	0.393	0.996	0.885
Average	0.850	0.972	0.970	0.983	0.644	0.984	0.901

Table 5
Percentage change in the calculated butanol production in response to a 5% increase in each parameter of reaction equations

	ED[a]	ID[b]	IAD[c]	Temporal profile in Fig. 2
$V_{max\,1}$	−1.52	−0.87	1.81	d
K_{m1}	1.11	0.66	1.27	c
K_{is1}	−0.28	−0.10	0.38	d
K_{ii1}	−0.09	−0.06	0.10	d
$V_{max\,2}$	0.01	0.02	0.02	
K_{m2}	0	−0.01	0.01	
$V_{max\,3}$	0.01	0.01	0.01	
K_{m3}	0	−0.01	0.02	
$V_{max\,4}$	0.01	0	0.01	
K_{m4}	0.01	0.01	0.01	
$V_{max\,5}$	0	0	0.01	
K_{m5}	0	0	0.01	
$V_{max\,6}$	0.01	0	0.01	
K_{m6}	0	0	0.01	
$V_{max\,7}$	0.56	0.58	0.58	a
K_{m7}	−0.34	−0.35	0.35	b
$V_{max\,8}$	−0.07	−0.05	0.08	d
K_{m8A}	0.07	0.04	0.08	c
K_{m8B}	0.05	0.03	0.05	c
$V_{max\,9}$	−0.07	−0.08	0.08	b
K_{m9}	0.07	0.08	0.08	a
$V_{max\,10}$	0.62	0.24	0.83	c
K_{m10}	−0.61	−0.27	0.81	d
$V_{max\,11}$	−0.04	−0.05	0.05	b
K_{m11}	0.04	0.04	0.04	a
$V_{max\,12}$	−0.52	−0.14	0.76	d
K_{m12}	0.49	0.11	0.73	c
K_{ii12}	−0.20	−0.11	0.25	d
$V_{max\,13}$	−0.01	−0.05	0.05	b
$V_{max\,14}$	0.97	0.92	0.92	a
K_{m14}	−0.93	−0.88	0.88	b
$V_{max\,15}$	−0.87	−0.84	0.84	b
K_{m15A}	0.84	0.81	0.81	a
K_{m15B}	0.75	0.73	0.73	a
$V_{max\,16}$	0	0	0	
K_{m16}	0	0	0	
$V_{max\,17}$	0.98	1.00	1.00	a
K_{m17}	−0.53	−0.54	0.54	b
K_{a17}	−0.16	−0.16	0.16	b
$V_{max\,18}$	−1.02	−1.04	1.04	b
K_{m18}	0.83	0.85	0.85	a
$V_{max\,19}$	1.06	1.10	1.10	a
K_{m19}	−0.88	−0.91	0.91	b
K_{ii19}	0.05	0.05	0.05	a
K_{a19}	−0.26	−0.26	0.26	a

[a] Endpoint deviation of butanol production.
[b] Integral deviation of butanol production.
[c] Integral absolute deviation of butanol production.

Table 6
Percentage change in the calculated butanol production in response to a 5% decrease in each parameter of reaction equations

	ED[a]	ID[b]	IAD[c]	Temporal profile in Fig. 2
$V_{max\,1}$	1.62	0.87	1.92	c
K_{m1}	−1.15	−0.71	1.31	d
$V_{max\,14}$	−1.03	−0.98	0.98	b
K_{m14}	0.96	0.91	0.91	a
$V_{max\,15}$	0.89	0.87	0.87	a
K_{m15A}	−0.89	−0.86	0.86	b
K_{m15B}	−0.80	−0.78	0.78	b
$V_{max\,17}$	−1.05	−1.08	1.08	b
K_{m17}	0.55	0.55	0.55	a
$V_{max\,18}$	1.04	1.07	1.07	a
K_{m18}	−0.89	−0.91	0.91	b
$V_{max\,19}$	−1.16	−1.19	1.19	b
K_{m19}	0.91	0.93	0.93	a

[a] Endpoint deviation of butanol production.
[b] Integral deviation of butanol production.
[c] Integral absolute deviation of butanol production.

As can be seen from Table 5, the greatest impact on ED of butanol is R_1 in Fig. 1. The increase in r_1 caused negative ED and ID which means negative contribution to butanol production; a 5% increase in $V_{max\,1}$ resulted in a 1.52% and 0.87% decrease in ED and ID, respectively and 1.81% increase in IAD (temporal profile (d) in Fig. 2). The second impact reaction on ED of butanol was R_{19} in Fig. 1; a 5% increase in $V_{max\,19}$ resulted in a 1.06%, 1.10%, and 1.10% increase in ED, ID, and IAD, respectively (temporal profile (a) in Fig. 2), which showed positive impact of $V_{max\,19}$ on butanol production. R_{14}, R_{15}, R_{17}, and R_{18} in Fig. 1 had also great impact on ED of butanol. R_{15} and R_{17} represent the butyrate utilization by CoAT and the reverse reaction of butyrate production, respectively. As shown in Table 5, the sensitivity of butanol production by a 5% increase in r_{15} was negative while the sensitivity in r_{17} was positive; a 5% increase in $V_{max\,15}$ resulted in a 0.87% and 0.84% decrease in ED and ID and 0.84% increase in IAD, respectively (temporal profile (b) in Fig. 2), and a 5% increase in $V_{max\,17}$ resulted in a 0.98%, 1.00%, and 1.00% increase in ED, ID, and IAD, respectively (temporal profile (a) in Fig. 2). Comparing the result of r_{15} with that of r_{17}, reassimilation of butyrate by R_{17} was more important for high butanol production than that by R_{15}. We could not find the case of butanol behaviors which belong to the temporal profiles (e) and (f) in Fig. 2. Furthermore, sensitivity analysis was carried out by 5% decrease in the kinetic parameters which has great impact on butanol production (R_1, R_{14}, R_{15}, R_{17}, R_{18}, and R_{19}). As shown in Table 6, the absolute values of ED and ID were almost same as those in the case of a 5% increase of the parameters.

4. Discussion

Modeling of metabolic pathways is useful for the system analyses (Berríos-Rivera et al., 2002; Granström et al., 2002; Koffas et al., 2003; Woldman and Appling, 2002) and optimization of cultivation processes (Shimizu et al., 1999). Many of the computer simulations have employed either dynamic simulation or MFA to predict the behavior of metabolic pathways. Since MFA provides only a snapshot of the pathway properties at a steady state under specific environmental conditions, it cannot provide information on time-dependent changes in each flux. On the other hand, the kinetic simulation model represented by a set of simultaneous differential equations provides temporal evolution of pathway properties, although collecting a complete set of kinetic parameters is extremely difficult. Focused on ABE production, there is no report on the development of a kinetic

simulation model for describing the dynamic behaviors (temporal responses) of target metabolites such as glucose, acetone, butanol, acetate, butyrate, and biomass. In this study, we have first proposed a novel kinetic simulation model that describes such dynamic behaviors and have carried out a sensitivity analysis to assess its validity and to reveal which pathways have impact on high production of butanol.

Kinetic parameters were estimated by the heuristic searching method to realize the experimentally obtained time-course data of glucose, acetone, butanol, acetate, butyrate, and biomass for the initial glucose concentration of 70.6 mM. Furthermore, to confirm the validity of the developed model, we next examined whether the designed models could describe the experimentally obtained time-course data for initial glucose concentrations of 36.1, 122, and 295 mM as well. As shown in Figs. 6 and 7, and Table 4, the proposed model for ABE production with fixed values of kinetic parameters (Model III) could describe the dynamic behaviors of target metabolites (0.901 of r^2), even when the initial concentration of glucose varied between 36.1 and 295 mM. Even though this model does not consider ATP- and NADH-balances, it is one of the best candidates for kinetic simulation of metabolic pathways in ABE production.

Sensitivity analysis by the kinetic simulation model can reveal which pathways have most impact on high production of target products. Sensitivity analysis was carried out to assess the impact on endpoint butanol production, amount of butanol production, and butanol productivity with a 5% change in each kinetic parameter in rate equations. As shown in Table 5, a 5% increase in kinetic parameters ($V_{\max 1}$, K_{m1}) at R_1 had a greatest negative impact on the butanol production. The values of IAD were higher than the absolute value of ID (temporal profile (d) in Fig. 2), indicating that 5% increase in the parameters of R_1 has positive impact on the amount of butanol production during early phase in cultivation and negative impact on butanol productivity during late phase in cultivation. Furthermore, these results indicated that early production of butanol had a negative effect on butanol production.

Butyrate reassimilation is generally considered to occur via CoAT (R_{15}) and the reverse pathway of butyrate production (R_{17}) (Jones and Woods, 1986; Desai et al., 1999). So, we carried out the sensitivity analysis to reveal which pathways are effective for butanol production. The sensitivity of butanol production by a 5% increase of $V_{\max 17}$ in r_{17} was positive and the temporal profile belongs to (a) in Fig. 2, while the sensitivity in r_{15} was negative and the temporal profile belongs to (b) in Fig. 2 (Table 5). The sensitivity of butanol production by a 5% decrease of $V_{\max 15}$ was positive and the temporal profile belongs to (a) in Fig. 2 (Table 6). Furthermore, a 5% decrease in $V_{\max 15}$ had a negative impact on acetone production (data not shown here). These results indicated that decrease of acetone production was responsible for the butanol production. Comparing the result of r_{15} and that of r_{17}, reassimilation by R_{17} was more important and more preferable for butanol production than that by R_{15}. Therefore, we could predict which pathway have more impact on the higher butanol production by using developed model. Based on the results in Tables 5 and 6, Table 7 is summarized the estimated manipulation strategy of kinetic parameters for the higher butanol production.

Table 7
Estimated manipulation strategy for the higher butanol production

Reaction number	Kinetic parameter	Increase	Decrease	Temporal profile
R_1	$V_{\max 1}$		○	c
	K_{m1}	○		c
R_{14}	$V_{\max 14}$	○		a
	K_{m14}		○	a
R_{15}	$V_{\max 15}$		○	a
	K_{m15A}	○		a
	K_{m15B}	○		a
R_{17}	$V_{\max 17}$	○		a
	K_{m17}		○	a
R_{18}	$V_{\max 18}$		○	a
	K_{m18}	○		a
R_{19}	$V_{\max 19}$	○		a
	K_{m19}		○	a

The main focus of metabolic engineering is metabolic pathways and its goal is the optimization of the yield of some desired metabolites. The optimization aims to identify the best possible outcome, and from a mathematical viewpoint, outcome is a value of some function – often called the objective function – and the best possible value of the outcome is the maximum or minimum of the objective function. In other words, optimal control is to estimate the values of time-dependent control variables for maximizing or minimizing the objective function. What is the best optimal strategy for maximizing butanol production? Related to this problem, we have analyzed the time-sliced metabolic flow of each pathway in ABE production. In addition, once the kinetic parameters in the dynamic simulation model are fixed, we can examine the time-variant changes in every metabolic flow during the transient time period, which lead us to the prediction on the target pathways to be controlled.

References

Bailey, J.E., 1991. Toward a science of metabolic engineering. Science 252, 1668–1675.

Berríos-Rivera, S.J., Bennett, G.N., San, K.Y., 2002. The effect of increasing NADH availability on the redistribution of metabolic fluxes in *Escherichia coli* chemostat cultures. Metab. Eng. 4, 230–237.

Boynton, Z.L., Bennett, G.N., Rudolph, F.B., 1994. Intracellular concentrations of coenzyme A and its derivatives from *Clostridium acetobutylicum* ATCC 824 and their roles in enzyme regulation. Appl. Environ. Microbiol. 60, 39–44.

Desai, R.P., Harris, L.M., Welker, N.E., Papoutsakis, E.T., 1999. Metabolic flux analysis elucidates the importance of the acid-formation pathways in regulating solvent production by *Clostridium acetobutylicum*. Metab. Eng. 1, 206–213.

Gear, C.W., 1971. Numerical Initial Value Problems in Ordinary Differential Equations. Prentice-Hall, New Jersey.

Granström, T., Aristidou, A.A., Leisola, M., 2002. Metabolic flux analysis of *Candida tropicalis* growing on xylose in an oxygen-limited chemostat. Metab. Eng. 4, 248–256.

Hodge, D.B., Karim, M.N., 2002. Modeling and advanced control of recombinant *Zymomonas mobilis* fed-batch fermentation. Biotechnol. Prog. 18, 572–579.

Ishizaki, A., Michiwaki, S., Crabbe, E., Kobayashi, G., Sonomoto, K., Yoshino, S., 1999. Extractive acetone–butanol–ethanol fermentation using methylated crude palm oil as extractant in batch culture of *Clostridium saccharoperbutylacetonicum* N1-4 (ATCC 13564). J. Biosci. Bioeng. 87, 352–356.

Jones, D.T., Woods, D.R., 1986. Acetone–butanol fermentation revisited. Microbiol. Rev. 50, 484–524.

Koffas, M.A.G., Jung, G.Y., Stephanopoulos, G., 2003. Engineering metabolism and product formation in *Corynebacterium glutamicum* by coordinated gene overexpression. Metab. Eng. 5, 32–41.

Lee, T.M., Ishizaki, A., Yoshino, S., Furukawa, K., 1995. Production of acetone, butanol and ethanol from palm oil waste by *Clostridium saccharoperbutylacetonicum* N1-4. Biotechnol. Lett. 17, 649–654.

Okamoto, M., Sakai, T., Hayashi, K., 1988. Biochemical switching device realizing McCulloch–Pitts type equation. Biol. Cybern. 58, 295–299.

Okamoto, M., Morita, Y., Tominaga, D., Tanaka, K., Kinoshita, N., Ueno, J., Miura, Y., Maki, Y., Eguchi, Y., 1997. Design of virtual-labo-system for metabolic engineering: development of biochemical engineering system analyzing tool-kit (BEST-KIT). Comput. Chem. Eng. 21, 745–750.

Papoutsakis, E.T., 1984. Equations and calculations for fermentations of butyric acid bacteria. Biotechnol. Bioeng. 26, 174–187.

Rizzi, M., Baltes, M., Theobald, U., Reuss, M., 1997. In vivo analysis of metabolic dynamics in *Saccharomyces cerevisiae*: II. mathematical model. Biotechnol. Bioeng. 55, 592–608.

Sekiguchi, T., Okamoto, M., 2006. WinBEST-KIT: Windows-based biochemical reaction simulator for metabolic pathways. J. Bioinform. Comput. Biol. 4, 621–638.

Shimizu, H., Takiguchi, N., Tanaka, H., Shioya, S., 1999. A maximum production strategy of lysine based on a simplified model derived from a metabolic reaction network. Metab. Eng. 1, 299–308.

Soni, B.K., Das, K., Ghose, T.K., 1987. Inhibitory factors involved in acetone–butanol fermentation by *Clostridium saccharoperbutylacetonicum*. Curr. Microbiol. 16, 61–67.

Stephanopoulos, G., Vallino, J.J., 1991. Network rigidity and metabolic engineering in metabolite overproduction. Science 252, 1675–1681.

Tashiro, Y., Takeda, K., Kobayashi, G., Sonomoto, K., Ishizaki, A., Yoshino, S., 2004. High butanol production by *Clostridium saccharoperbutylacetonicum* N1-4 in fed-batch culture with pH-stat continuous butyric acid and glucose feeding method. J. Biosci. Bioeng. 98, 263–268.

Vallino, J.J., Stephanopoulos, G., 1993. Metabolic flux distributions in *Corynebacterium glutamicum* during growth and lysine overproduction. Biotechnol. Bioeng. 41, 633–646.

Woldman, Y., Appling, D.R., 2002. A general method for determining the contribution of split pathways in metabolite production in the yeast *Saccharomyces cerevisiae*. Metab. Eng. 4, 170–181.

Yoshimura, J., Shimonobou, T., Sekiguchi, T., Okamoto, M., 2003. Development of the parameter-fitting module for web-based biochemical reaction simulator BEST-KIT. Chem-Bio. Inform. J. 3, 114–129.